Boron-Doped Diamond Functionalization by an Electrografting - Alkyne-Azide Click Chemistry Sequence

W.S. Yeap[1*], M.S. Murib[1], W. Cuypers[1], X. Liu[2], B. van Grinsven[1], M. Ameloot[3], M. Fahlman[2], P. Wagner[1,4], W. Maes[1,4], and K. Haenen[1,4*]

[1] Hasselt University, Institute for Materials Research (IMO), B-3590 Diepenbeek, Belgium
[2] Linköping University, Department of Physics, Chemistry and Biology, S-58183 Linköping, Sweden
[3] Hasselt University, BIOMED, Agoralaan, B-3590 Diepenbeek, Belgium
[4] IMEC vzw, IMOMEC, B-3590 Diepenbeek, Belgium

* To whom correspondence should addressed.
Tel.: +32 11 26 8826; fax: +32 11 26 8899
E-mail address: wengsiang.yeap@uhasselt.be (W.S. Yeap)
E-mail address: ken.haenen@uhasselt.be (K. Haenen)

Keywords: azide, boron-doped diamond, click chemistry, diazonium electrografting, DNA

Abstract:

A straightforward protocol for the covalent functionalization of boron-doped diamond electrodes with either ferrocene or single-stranded deoxyribonucleic acid (ss-DNA) is reported. The functionalization method is based on a combination of diazonium salt electrografting and click chemistry. An azide-terminated organic layer is first electrografted on the diamond surface by electrochemical reduction of 4-azidophenyldiazonium chloride. The azidophenyl-modified surface then reacts rapidly and efficiently with molecules bearing a terminal alkyne moiety by means of a Cu(I)-catalyzed alkyne-azide cycloaddition. Covalent attachment of ferrocene moieties was analyzed by means of X-ray photoelectron spectroscopy (XPS) and cyclic voltammetry (CV), whereas impedance spectroscopy was applied for the characterization of the immobilized DNA.

1. Introduction

Chemical Vapor Deposition (CVD) diamond recently receives great interest, both in science and technology.[1] The large attention for this material can be attributed to its outstanding properties such as biocompatibility,[2] chemical inertness, hardness and excellent thermal conductivity.[3] Synthetic CVD diamond can be boron-doped during its growth and shows p-type conductivity. In case of heavy B-doping, for concentrations above ~3 x 10^{20} cm^{-3}, metal-like conductivity is observed.[4] Boron-doped diamond shows a negligible rate of water electrolysis over a wide potential

range. Due to this wide potential window, CVD diamond surfaces are regarded as appealing electrodes.[5]

Another particular advantage of CVD diamond surfaces is the fact that surface functionalization can be readily achieved. Various strategies have been successfully applied to derivatize diamond surfaces.[6] The well-known photochemical surface modification using vinyl derivatives is a promising method for stable immobilization of molecular monolayers linked to the diamond substrate by C-C bonds.[7] The mechanism proposed for such photochemical modification involves a photoemission-induced radical reaction, possibly enabled by the negative electron affinity of hydrogen-terminated diamond surfaces.[8] Even though this method is widely accepted, it requires long reaction times and an inert atmosphere. Surface functionalization through esterification on UV-ozone oxidized diamond, as demonstrated by the group of Boukherroub and Szunerits,[9,10] allows molecules bearing carboxylic acid end groups to attach on diamond surfaces. It is, however, quite hard to achieve a homogenous hydroxyl layer on the diamond surface, as UV-ozone oxidation usually creates other oxygen functionalities as well, such as carboxylic and carbonyl moieties.[11] One-step functionalization of amine derivatives on diamond surfaces was recently demonstrated by Agnes *et al*.[12] This rapid new grafting protocol is based on the high affinity of hydrogenated diamond towards primary amines. However, as stated, this procedure is limited to the coupling of (bio)molecules bearing a primary amine group. Several groups have also demonstrated the coupling of arenediazonium salts onto diamond surfaces,[13] either by electrografting[14,15] or spontaneous grafting.[16] Electrografting is more attractive since it requires a shorter reaction time.[15] In general, this potential assisted method offers several advantages: i) an instantaneous surface modification, generally requiring only a few seconds for the formation of a saturated monolayer; ii) it does not require an inert atmosphere for efficient reaction; and iii) an easy control over the functionalization degree (i.e. surface coverage).[15] Electrografting on diamond surfaces has already been demonstrated for a variety of substituted aryl derivatives,[13] but not for azidophenyldiazonium salts.

Recently, the search for more efficient and controlled strategies for the functionalization of conductive surfaces, at the molecular level, with biological,[17] redox-active,[18] or photo/chemical sensitive molecules has become a central interest in the development of molecular electronics,[19] energy conversion systems,[20] and

chemical or biological sensors.[21] It has, however, been proven difficult to successfully realize the formation of these materials due to their inherent structural and functional properties.[22] Moreover, most coupling methods are hampered by the difficulty to introduce the required reactive groups, a lack of specificity, or a low yield.[23] Ligation strategies can offer a solution by interacting with specific kinds of functional groups. Click chemistry reactions can be seen as "the most advanced examples" providing a set of powerful, highly reliable and selective reactions.[22] The copper(I)-catalyzed alkyne-azide cycloaddition (CuAAC) reaction – 1,2,3-triazole formation through classical Huisgen 1,3-dipolar cycloaddition – is one of the most popular and renown click reactions.[24] This heterogenous coupling strategy was found to be fast, reproducible, with a minimum of side reactions, and highly tolerant to diverse reaction conditions. Click reactions have already been tested on various surfaces. For example, Arnold *et al.* recently demonstrated the clicking of 5-azidofluorescein to 4-(trimethylsilyl)ethynylstyrene polymer brushes that were grown on a silicon surface.[25] Grabosch *et al.* presented a 'dual click' strategy for the fabrication of bioselective glycosylated self-assembled monolayers as glycocalyx models.[26] They showed that their click reaction provides a rather mild surface immobilization with excellent coupling yields, versatility, regioselectivity, functional group tolerance, and stability of the catalytic process in different solvents and pHs.

In this work, we report on the modification of boron-doped CVD-grown diamond electrodes by electrografting an azidophenyl layer on the diamond surface through electrochemical reduction of the corresponding (*in situ* generated) 4-azidophenyldiazonium chloride salt, and subsequent chemoselective CuAAC coupling of terminal alkyne-bearing molecules. The surface coverage with reactive azide moieties was quantified electrochemically through complementary coupling of a simple redox-active probe, i.e. ethynylferrocene. Finally, the utility of the azide-functionalized diamond electrode for fast and efficient covalent attachment of a ss-DNA probe was demonstrated by reaction with an alkyne-functionalized DNA probe. The resulting device and its capability to work as a DNA-based sensor were evaluated by impedance spectroscopy. Due to the highly chemoselective nature of the alkyne-azide click reaction, azide-terminated boron-doped diamond electrodes can be regarded as a generic platform, providing a reliable coverage, for coupling with a wide range of ethynyl-terminated species of interest for various (sensing) applications.

2. Results and discussion

2.1. Electrografting of phenylazide groups

As shown in Figure 1, 4-azidophenyldiazonium chloride is formed *in situ* by diazotization when hydrochloric acid and sodium nitrite solutions are added to 4-azidoaniline.[14] Application of a potential reduces the diazonium salt to a radical species.[15] As the density and thickness of the functionalized layer depend on the potential applied,[15,27] we analyzed the effect of the potential on the formation of the 4-azidophenyl layer.

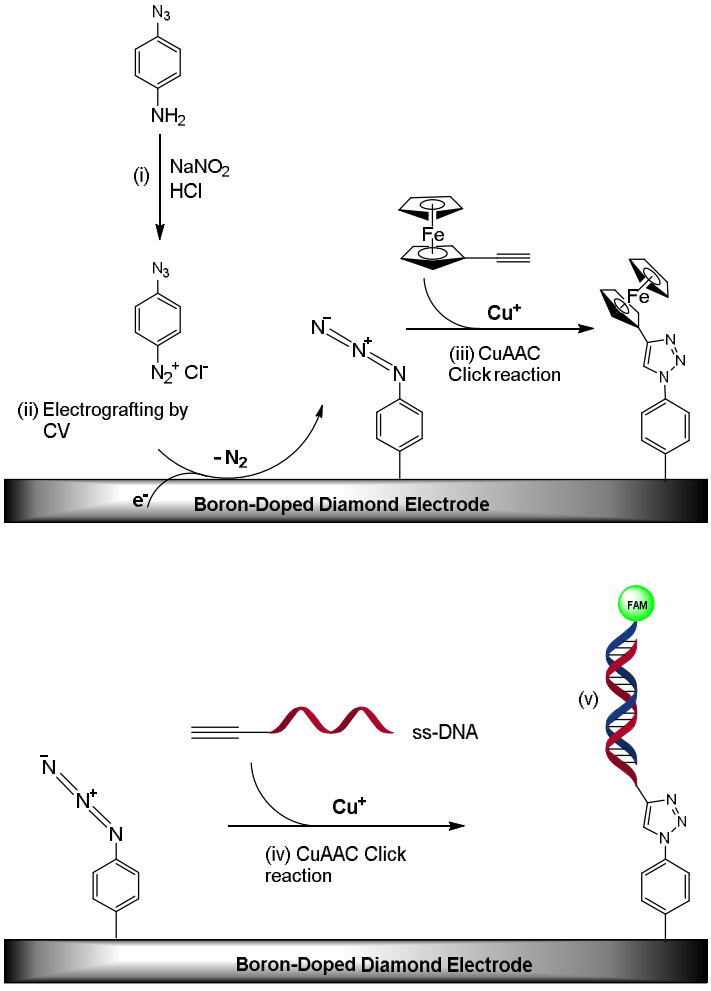

Figure 1. Illustration of the multistep functionalization of boron-doped diamond electrodes: i) Diazotization; ii) Electroreduction of the diazonium salt for electrografting of phenylazide molecules; iii) Cu(I)-catalyzed Huisgen 1,3-dipolar cycloaddition between the immobilized phenylazide molecules and ethynylferrocene; iv) Cu(I)-catalyzed Huisgen 1,3-dipolar cycloaddition between the immobilized phenylazide molecules and ss-DNA; v) Hybridization with fluorescein-labeled (FAM) target DNA molecules.

Commercially available freestanding electrochemical grade boron-doped microcrystalline CVD diamond plates from Element Six (E6) and home-grown boron-doped nanocrystalline diamond (NCD) thin films were used in this work. The latter were grown on fused silica substrates, which make them not suitable for our impedance measurements later. As a result, the former is chosen for the impedance measurements and are referred to as B:MCD. The in-house deposited material is named as B:NCD in this article. Figure 2 shows the cyclic voltammograms of three boron-doped nanocrystalline diamond (B:NCD) samples that underwent electrografting. Each sample was subjected to a different potential scan (cfr. Table 1, exp. section). The cyclic voltammogram of diamond sample EG 1 (Figure 2a) did not show any peak that can be related to the electroreduction of the diazonium salt, indicating that the diamond sample was not functionalized. When we applied a more negative potential (up to -0.8 V, sample EG 2), a broad irreversible reduction peak appeared during the first scan, which disappeared on the second scan (as indicated by the arrow in Figure 2b). This reduction peak can be related to the formation of radicals upon electroreduction of the diazonium salt.[14,15] The disappearance of the reduction peak during the second scan (Figure 2b, blue line) is due to the passivation of the diamond surface by the electrochemically grafted organic layer, blocking the access of the diazonium cations to the electrode surface.[15]

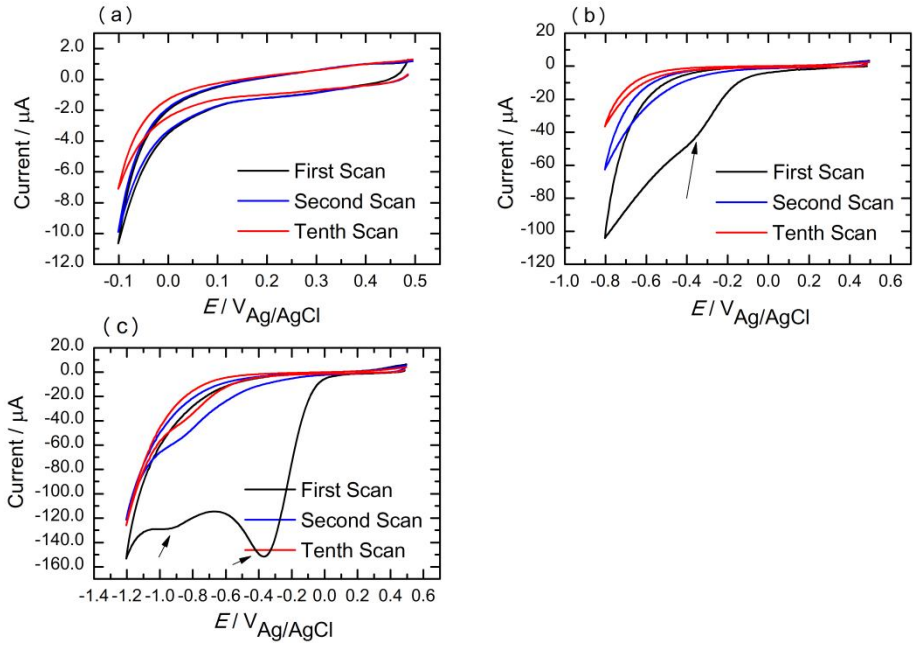

Figure 2. *In situ* electrochemical generation of 4-azidoaniline-derivatized aryl diazonium salts onto hydrogenated B:NCD samples, showing first, second and tenth

CV reduction cycles with applied potential between a) +0.5 and -0.1 V; b) +0.5 and -0.8 V; c) +0.5 and -1.2 V at a scan rate of 100 mVs^{-1}.

When an even more negative potential (up to -1.2 V, sample EG 3) was applied, two reduction peaks clearly appeared (Figure 2c). Besides the broad irreversible reduction peak at -0.4 V, which indicates the presence of radicals, a smaller reduction peak appeared at around -0.9 V. Cycling to a more negative potential leads to the formation of anions by further reduction of the formed radicals.[15]

2.2. Clicking ferrocene groups to phenylazide-functionalized B:NCD

4-Ethynylferrocene was chosen as a model molecule to couple to the 4-azidophenyl-functionalized B:NCD with the intention to confirm the presence of the phenylazide groups and to demonstrate that the click reaction can effectively be carried out on this functionalized surface. The three different diamond samples EG 1–3 were all subjected to a CuAAC click reaction with ethynylferrocene in the presence of $CuSO_4.5H_2O$ and L-ascorbic acid (L-AA). The presence of the ferrocene groups after the click reaction was probed by CV in a solution of 0.1 M tetrabutylammonium hexafluorophosphate ($TBAPF_6$) in acetonitrile (ACN). As shown in Figure 3, ferrocene groups could be observed for the EG 2 (red line) and EG 3 (blue line) diamond samples, with a redox peak $E°$ = ~ 0.19 V *vs.* $Ag/AgNO_3$ and a peak separation of ΔE = 37 mV (for both samples). The bound ferrocene moieties show a similar redox potential as compared to a ferrocene-modified crystalline silicon ($E°$ = ~ 0.15 V *vs.* Ag/AgCl) electrode.[28] It is known that the width of the current peaks depends strongly on the distribution of the individual ferrocenes. For identical and non-interacting ferrocenes, the ideal full width at half-maximum (FWHM) is 90 mV.[29] The EG 2 and EG 3 samples show an FWHM of 125 and 127 mV, respectively. From these values, we conclude that the ferrocene entities formed are not significantly aggregated and are subject to almost identical redox conditions.[29]

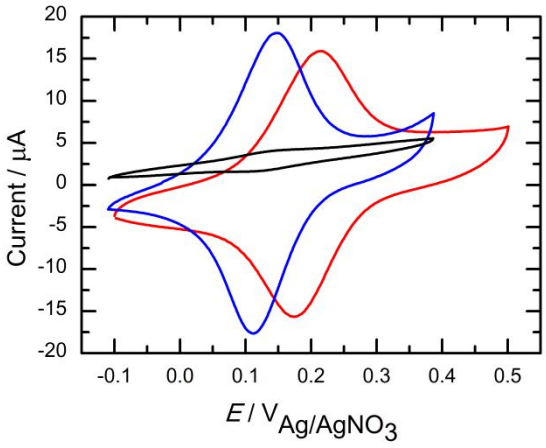

Figure 3. Cyclic voltammograms of diamond samples EG 1 (black line), EG 2 (red line), and EG 3 (blue line) after click reaction with ethynylferrocene in $TBAPF_6$ (0.1 M in ACN), scan rate 100 mVs^{-1}.

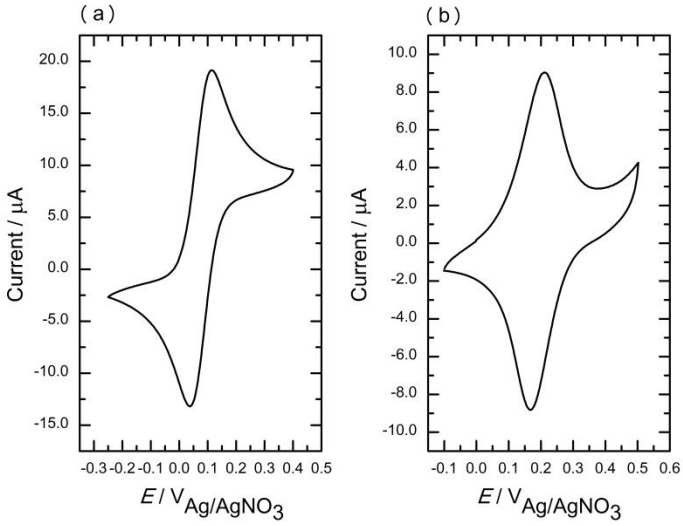

Figure 4. Cyclic voltammograms of (a) ferrocene in $TBAPF_6$ (0.1 M in ACN) at a Pt-disc electrode, and (b) a ferrocene-terminated -B:NCD surface (EG 2) in $TBAPF_6$ (0.1 M in ACN) (scan rate 100 mVs^{-1}).

The anodic-cathodic peak separation gives the first evidence that the ferrocene groups are covalently bound onto the diamond surface after the click reaction. As shown in Figure 4b, the peak separation (ΔE_p) for the EG 2 sample was 37 mV at a potential sweep rate of 100 mVs^{-1}, much smaller than the peak separation for a diffusion-controlled one-electron reversible redox system (Figure 4a, 57 mV).[30] Similar results were obtained as compared to a ferrocene-modified diamond electrode prepared via a photochemical method.[31] The electron transfer mechanism for surface-bound redox active species depends on charge-transfer rather than diffusion-controlled kinetics.[30]

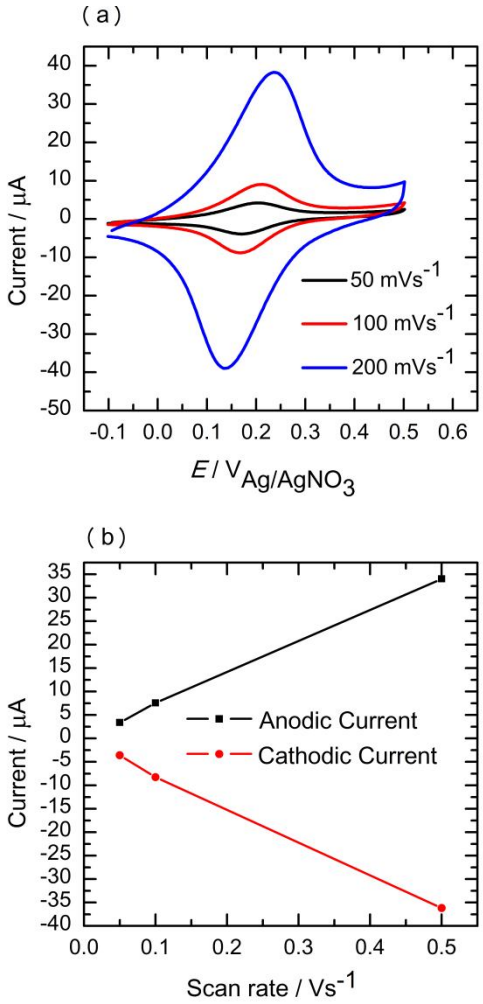

Figure 5. (a) Cyclic voltammograms of a ferrocene-functionalized HG-BDD surface in $TBAPF_6$ (0.1 M in ACN), scan rate 50 mVs^{-1} (black), 100 mVs^{-1} (red), and 200 mVs^{-1} (blue). (b) Peak current as a function of scan rate for anodic (■) and cathodic (●) peak currents.

An analysis of the change in peak currents as a function of scan rate allows additional assessment of the fact that the ferrocene groups are surface-bound rather than physically adsorbed. Figure 5b shows that there is a linear relationship between either the anodic or cathodic peak current and the scan rate (v), suggesting a fast charge transfer process of the bonded ferrocene molecules with the electrode surface.[10,30,31] This characteristic points to a surface redox process controlled by charge transfer kinetics. A similar behavior has also been observed for ferrocenecarboxylic acid-modified single-crystal Si(111) surfaces[28] and ferrocene-based alkanethiol layers on gold.[32]

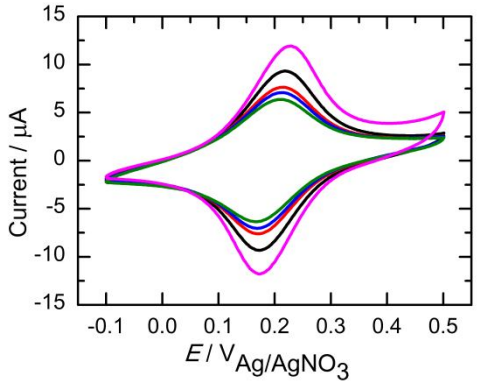

Figure 6. Cyclic voltammograms of ferrocene-functionalized B:NCD (EG 2) showing the 1st scan (pink line), 50th scan (black line), 100th scan (red line), 150th scan (blue line), and 200th scan (green line) in $TBAPF_6$ (0.1 M in ACN), scan rate 100 mVs^{-1}. The anodic peak height shows a decrease of 26% after 200 scans.

The electrochemical stability of the ferrocene-functionalized B:NCD sample (EG 2) was examined by successive potential cycling in $TBAPF_6$ (0.1 M in ACN) from -0.1 to +0.5 V *vs* $Ag/AgNO_3$ with a potential sweep rate of 100 mVs^{-1}. Figure 6 shows that the oxidation and reduction peaks are still clearly visible after 200 scans. Only a small decrease of the anodic peak height (~26%) is observed. This indicates that a strong covalent bond is formed between the ferrocene molecules and the 4-azidophenyl-functionalized diamond surface.

The ferrocene coverage (Γ, molecules cm^{-2}) of the diamond electrode was estimated from the charge of the CV anodic peak, *Q*, assuming a one-electron reaction, using the following relationship;

$$\Gamma = QA / nFA \quad (1)$$

where $n = 1$ is the number of electrons transferred during the redox reaction, F is Faraday's constant, and A is the area of exposed diamond electrode (= 0.5 cm^2). The ferrocene coverage was determined to be 1.48 ± 0.5 x 10^{14} molecules per cm^2 for the EG 2 sample, comparable to the values reported previously.[10, 31] From this value and comparison to the value reported before,[30] we can conclude that a near to single monolayer of ferrocene entities is formed.

Water contact angle measurements were conducted to identify the macroscopic changes in the wetting properties of the diamond surface after each functionalization step. A hydrogen terminated diamond surface is hydrophobic with a water contact angle of θ = 110.6°. The water contact angle value decreased slightly to θ = 83.7° upon functionalization with the 4-azidophenyl layer. After clicking ferrocene groups to the phenylazide groups, the contact angle dropped further to θ = 73.9°.

2.3. X-ray photoelectron spectroscopy (XPS)

X-ray photoelectron spectroscopy is a valuable tool to evaluate the changes in the surface chemical composition and binding that have occurred during surface derivatization. Figure 7(i) displays the XPS survey spectrum of a hydrogenated B:NCD surface. It shows a main peak at 285 eV (C 1s) from the bulk diamond and a small peak at 532 eV (O 1s) due to the adsorption of oxygen on the surface.

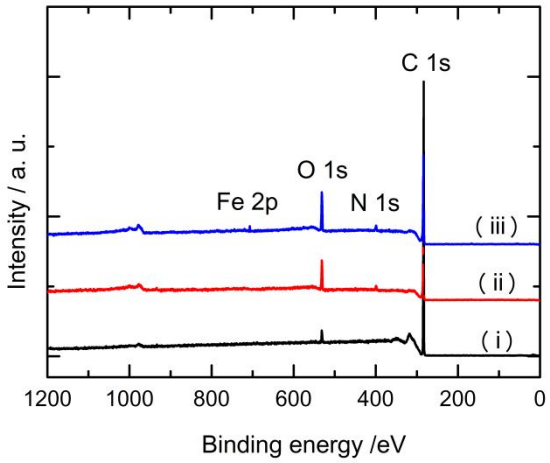

Figure 7. XPS spectra for (i) hydrogenated B:NCD, (ii) electrografted B:NCD, and (iii) electrografted B:NCD following click chemistry with ethynylferrocene.

After electrografting of the 4-azidophenyl groups, an additional small peak at ~ 400 eV was observed, in agreement with the chemical composition of the attached molecule (Figure 7(ii)). High-resolution XPS of the N 1s region of the 4-azidophenyl-functionalized B:NCD surface (Figure 8) showed a broad peak centered at ~ 400 eV and a second small peak centered at ~ 404 eV, suggesting the presence of chemically different nitrogen atoms. The central nitrogen atom of the azide group, with a characteristic peak at ~ 404 eV for the grafted electrode, has a low electron density and thus a higher binding energy.[33] XPS is particularly useful to monitor the click chemistry process as the intensity of this peak is greatly reduced after this reaction step. After clicking the ferrocene groups onto the 4-azidophenyl-functionalized B:NCD surface, the peak at ~ 404 eV disappeared almost completely and the peak at ~ 400 eV broadened (Figure 8, blue line). This can be seen as evidence for the transformation of the azide group into the 1,2,3-triazole unit attached to the terminal ferrocene. In addition, a high-resolution XPS scan of the Fe 2p region additionally demonstrated the presence of the ferrocene moieties on the B:NCD surface (Figure 9).

The Fe $2p_{3/2}$ and $2p_{1/2}$ peaks are observed at 707.7 and 720.6 eV, respectively. This indicates that the Fe moiety exists mainly in its +III oxidation state, in agreement with previously reported results on ferrocene groups anchored onto diamond[10] and silicon surfaces.[28]

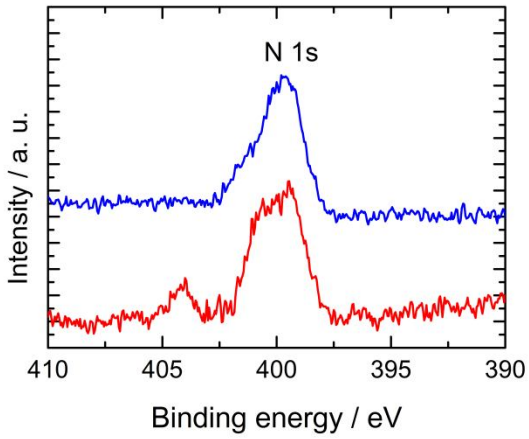

Figure 8. High-resolution XPS spectra of the N 1s region for electrografted B:NCD (red line), and electrografted B:NCD following click chemistry with ethynylferrocene (blue line).

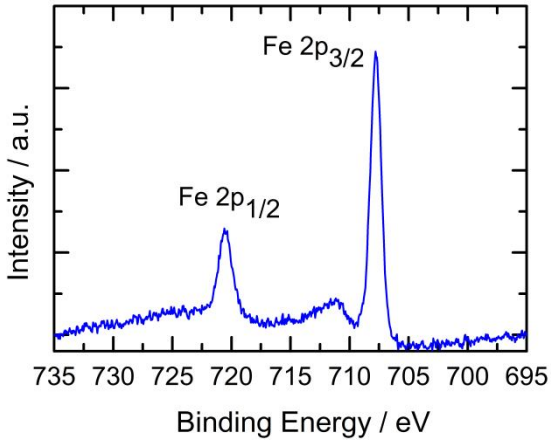

Figure 9. High-resolution XPS spectrum of the Fe 2p region for the electrografted B:NCD following click chemistry with ethynylferrocene.

2.4. Clicking an alkyne-terminated DNA probe onto phenylazide-functionalized B:MCD

The utility of the 4-azidophenyl-functionalized diamond electrode for fast and efficient attachment of a ss-DNA probe was demonstrated with the coupling of an alkynyl-derivatized ss-DNA probe followed by hybridization of the target DNA molecule (Figure 1). To avoid oxidative cleavage of the ss-DNA molecules by L-

ascorbic acid (L-AA), the DNA click reaction was carried out using CuBr and tris-(benzyltriazolylmethyl)amine (TBTA) instead of L-AA and $CuSO_4.5H_2O$.[34] The ss-DNA probe was first immobilized onto a 4-azidophenyl-functionalized B:MCD sample, followed by hybridization with fully complementary DNA. This hybridization process could be verified with confocal microscopy since the target DNA was labelled with 6-carboxyfluorescein (FAM). The B:MCD sample on which the immobilization protocol was carried out (as described above) showed an intense fluorescence signal (Figure 10(a)). This confirms the hybridization of the target DNA to the probe DNA attached by the click reaction. The black bar in Figure 10(b) was induced by photobleaching of the FAM fluorophore. On the other hand, no hybridization was observed for the B:MCD sample without phenylazide layer (Figure 10(c)).

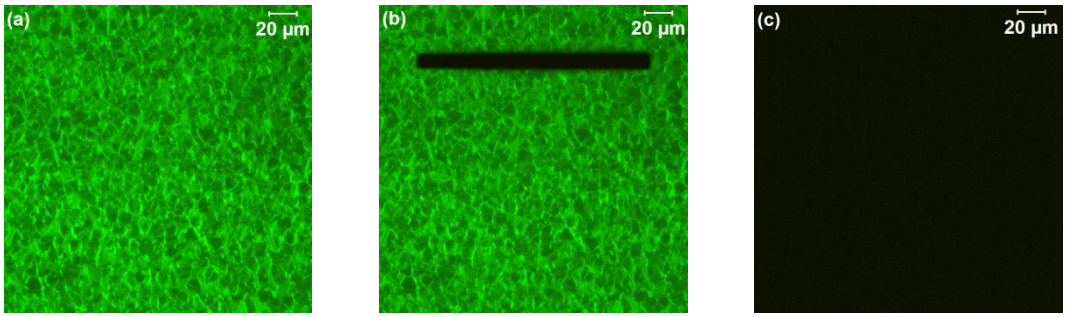

Figure 10. Confocal fluorescence images of B:MCD samples: (a) ss-DNA probe clicked to phenylazide-functionalized B:MCD and hybridized with FAM-tagged target DNA hybridized to the ss-DNA. (b) The black bar in the middle was induced by photobleaching of the FAM fluorophore. (c) ss-DNA probe reacted with bare hydrogenated B:MCD under the same click reaction conditions as for (a).

2.5. Impedance spectroscopy of phenylazide- and DNA-modified diamond surfaces

As the dynamics of electron transfer at the electrode interfaces are strongly influenced by the nature of the electrode surface, surface immobilization with (bio)molecules can significantly alter the interfacial electron transfer properties. Hence, the 4-azidophenyl-functionalized and DNA-modified diamond surfaces were evaluated by impedance spectroscopy.[35] The measurements were performed with a miniaturized impedance spectroscopy unit, as described before.[36] Figure 11 shows the Cole-Cole plot for bare B:MCD (red line) and phenylazide-grafted B:MCD (blue line). A lower admittance is observed for the 4-azidophenyl-functionalized B:MCD as compared to

the blank B:MCD. This is what is expected to be observed when an insulating organic molecular layer is chemically bonded onto an electrode.[33]

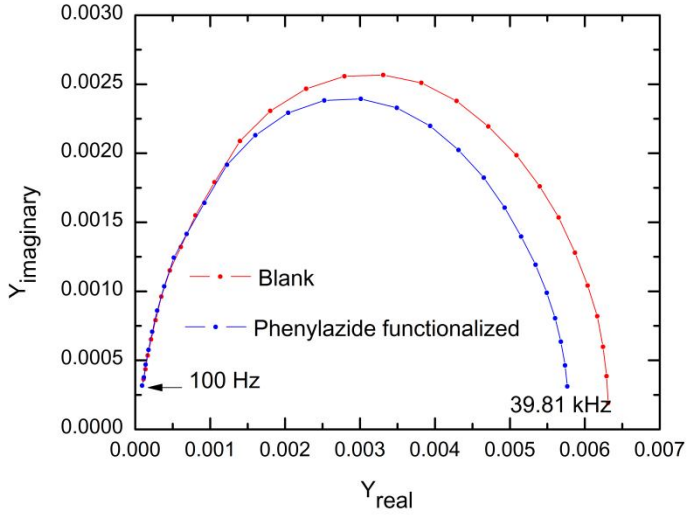

Figure 11. Cole-Cole plots showing the real and imaginary parts of the admittance for a blank B:MCD electrode (blue line) and a phenylazide-functionalized B:MCD electrode (red line).

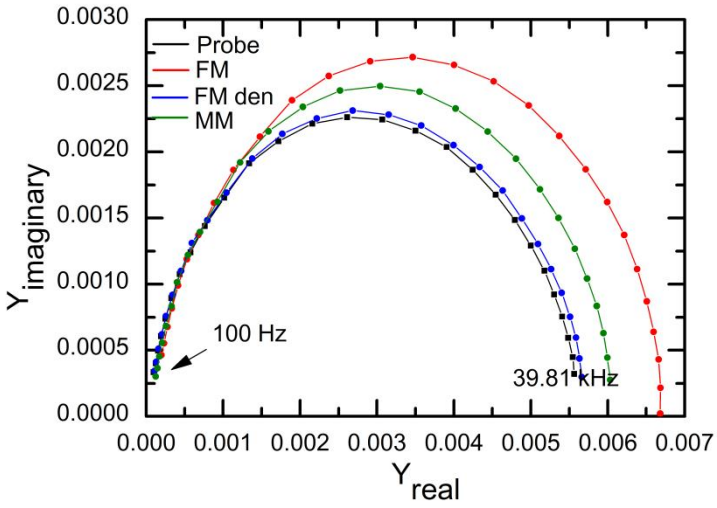

Figure 12. Cole-Cole plots showing the real and imaginary parts of the admittance for the B:MCD electrode, click immobilized with a ss-DNA molecule (black line), then hybridized with its fully complementary (FM, red line) and mismatch (MM, green line) DNA. After denaturation of the fully complementary DNA, the impedance signal falls back almost to its original position (FM den, blue line).

Figure 12 shows the Cole-Cole plots for the DNA-modified B:MCD sample in its different states in PBS (phosphate buffered saline) buffer solution. The 4-azidophenyl-functionalized B:MCD was modified first with ss-DNA by click chemistry and then analyzed by impedance spectroscopy (black line). After

hybridization with the target DNA, the impedance was measured again, resulting in an increase in Y_{real} and $Y_{imaginary}$ (red line). The hybridization-induced changes in Y_{real} and $Y_{imaginary}$ are quite apparent at frequencies above 1 kHz. These results agree well with previous findings showing that DNA molecules hybridizing at the interface induce a field effect in the diamond space-charge layer, lowering the impedance of the diamond.[35] Moreover, DNA is more conductive in its double-stranded form (i.e., after hybridization with a complementary sequence) compared to its single strand form.[37] Then, when the DNA was denatured by introducing 0.1 M NaOH into the flow cell, a third Cole-Cole plot was determined (blue line). Y_{real} and $Y_{imaginary}$ moved back toward their original positions. After denaturation, the impedance did not completely reverse to its initial state. The lack of this complete reversibility is yet unclear but might be due to the induced changes in the molecular layer by NaOH.[35,38] To determine the selectivity of DNA hybridization, the same ss-DNA modified B:MCD sample was hybridized with a non-complementary target DNA sequence (see Table 2, exp. section). Figure 12 (green line) clearly shows that the increase in the admittance due to hybridization with non-complementary DNA is smaller than observed upon hybridization with complementary DNA (red line).[35]

3. Conclusions

We have presented a simple yet efficient method to covalently attach functional organic molecules onto a boron-doped diamond electrode surface via a combination of diazonium electrografting and click chemistry. The functionalized diamond electrode was studied using cyclic voltammetry, impedance spectroscopy, and XPS to confirm the modification steps. This work also demonstrates, for the first time, the immobilization of DNA molecules on a diamond surface via CuAAC click chemistry. The DNA-click immobilized diamond electrode shows the possibility to be used as a DNA sensor. More in general, electrografted azidophenyl-functionalized diamond electrodes can be applied as a generic platform for coupling with a wide range of ethynyl-terminated species for various applications.

Experimental section

Chemicals and reagents

Sodium nitrite, sodium acetate, 4-azidoaniline hydrochloride, 4-ethynylferrocene, tetrabutylammonium hexafluorophosphate ($TBAPF_6$), L-ascorbic acid (L-AA), and $CuSO_4.5H_2O$ were used as received from Sigma Aldrich. All these products were used at their highest purity and used without further purification. The DNA sample was customized, synthesized and purchased from Base Click (Purity 95-98%). The kit used for clicking DNA on diamond was also purchased from Base Click. The kit contains CuBr, tris(benzyltriazolylmethyl)amine (TBTA) ligand and a solvent mixture of *tert*-butanol (*t*-BuOH) and dimethylsulfoxide (DMSO) in 1:3 v/v%. The solvents used for rinsing were of technical grade. Acetonitrile (ACN) used for the electrochemical work was of HPLC grade and was freshly distilled over CaH_2 prior to use. The water used for the electrochemical work was type 1 ultrapure water by Sartorius stedim biotech.

Preparation of the substrates

Commercially available freestanding electrochemical grade boron-doped microcrystalline CVD diamond plates from Element Six (E6) with [B] ~10^{21} cm^{-3}[39] and home-grown boron-doped nanocrystalline diamond (NCD) thin films were used in this work. The latter were grown on fused silica substrates, which make them not suitable for our impedance measurements. As a result, the former is chosen for the impedance measurements and are referred to as B:MCD. The in-house deposited material is named as B:NCD in this article. Sheet resistances (R_s), as measured by four-point probe measurements for B:NCD and B:MCD, were 1.06 and 207 Ω sq^{-1}, respectively. B:NCD films were grown by microwave plasma-enhanced chemical vapor deposition from methane/hydrogen mixtures (1% CH_4) in an ASTeX 6500 reactor. The growth conditions used were as follows: substrate temperature 700-900 °C, total gas flow of 500 sccm, total pressure in the reactor 30 Torr, microwave power 3500 W. Trimethylborane gas was added during the growth with a ratio of 10000 ppm B/C to ensure good electrical conductivity.[4] Based on previous experiments,[40] this ratio corresponds to a boron film concentration 10^{21} cm^{-3}. Prior to the diamond growth, the fused silica substrates were cleaned for 15 min each in RCA 1 (30% NH_3 + 30% H_2O_2 + H_2O; 1:1:5) and RCA 2 (37% HCl + 30% H_2O_2 + H_2O; 1:1:5) solutions at 90 °C. Following this, the cleaned fused silica substrates were

seeded with nanodiamond powder in water to improve the nucleation density.[4] After deposition, the diamond samples were allowed to cool down in the reactor for 30 min under a hydrogen flow. To remove any graphitic layers, the as-deposited diamond films were boiled in an acid mixture of 99% H_2SO_4 + 30% HNO_3 (3:1) at 90 °C for 30 min. After rinsing and sonicating thorougly with deionized water, the samples were subjected to hydrogenation. Figure 13 displays the scanning electron microscopy (SEM) images of (a) a typical as-grown 150 nm B:NCD thin film and (b) microcrystalline CVD diamond plates from Element Six (E6).

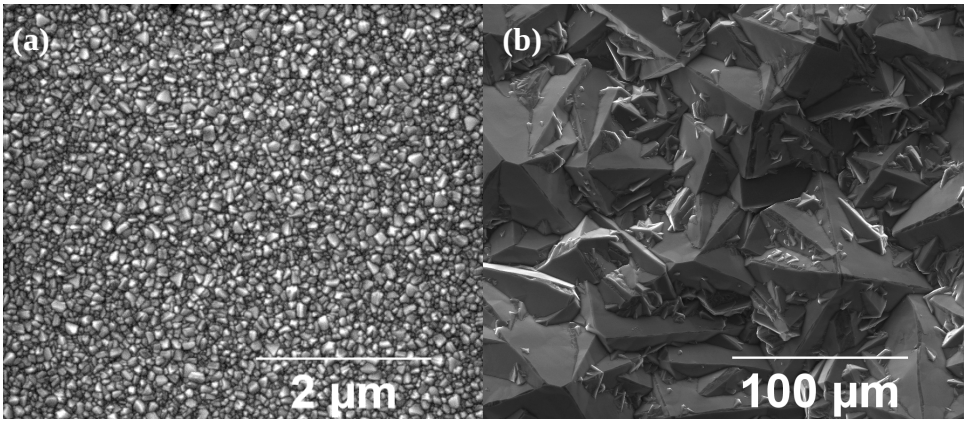

Figure 13. Typical SEM images of (a) B:NCD and (b) B:MCD films.

Hydrogenation on all diamond samples was performed using the same plasma-enhanced microwave CVD reactor that was used to grow the B:NCD. To create a hydrogen-terminated surface, all diamond samples were treated with hydrogen plasma under the following conditions: i) 500 sccm of hydrogen flux, 30 Torr reactor pressure with a 3500 W microwave power for 2 min; ii) 500 sccm of hydrogen flux, 15 Torr reactor pressure with a 2500 W microwave power for 5 min. At the end of the plasma treatment, the microwave power was switched off and the samples were allowed to cool down under hydrogen flux for 40 min. This hydrogenation step ensures full hydrogen termination and also serves to minimize dandling bonds.[41]

In situ generation of the diazonium salt

4-Azidoaniline (10 mg, 58.6 µmol) was used for the derivatization of the hydrogen-terminated diamond samples. It was diazotized with an equimolar amount of $NaNO_2$ (4 mg, 58.6 µmol).[13] It was first dissolved in a N_2-purged 0.5 M HCl solution (9.5 mL). Thereafter, 0.1 M $NaNO_2$ solution (0.5 mL) was added, bringing the final concentration to 5 mM. This electrolytic solution was then used for the electrografting procedure by means of cyclic voltammetry (CV).

Electrografting of the phenylazide groups

Functionalization of the diamond surface with 4-azidophenyl groups via electrochemical reduction of the *in situ* generated diazonium salt was carried out by CV.[14] The electrografting reactions were performed with an Autolab PGSTAT30 potentiostat **(**Eco Chemie B.V.) and controlled by the GPES Manager program. A one-compartment electrochemical cell was used with three-electrode configuration. The working electrode was a hydrogen-terminated diamond electrode. A platinum wire and $Ag/AgCl/KCl_{(sat)}$ electrodes were used as the counter and reference electrodes, respectively. All potentials are reported versus this reference electrode at room temperature. Half of the diamond sample was immersed in the reaction solution for larger area functionalization. Optimization of the electrografting process was carried out with B:NCD. As outlined above, 5 mM of 4-azidoaniline was diazotized with an equimolar amount of $NaNO_2$ in a N_2-purged HCl solution which was directly used for cyclic voltammetric scanning with 3 different potentials [+0.5 to -0.1 V (vs Ag/AgCl); +0.5 to -0.8 V (vs Ag/AgCl) and +0.5 to -1.2 V (vs Ag/AgCl)] at a scan rate of 100 mV/s for 10 scans. After the modifications, the B:NCD samples were rinsed with and sonicated in ultrapure water. Finally, these samples were dried by means of a nitrogen flow. The samples are referred to as listed in Table 1.

Table 1. B:NCD samples and their sample codes.

Applied potential	Sample code
+0.5 to -0.1 V (vs Ag/AgCl)	EG 1
+0.5 to -0.8 V (vs Ag/AgCl)	EG 2
+0.5 to -1.2 V (vs Ag/AgCl)	EG 3

B:MCD was derivatized with phenylazide groups with a single fixed potential (+0.5 to -0.8 V vs Ag/AgCl).

Clicking ferrocene groups to phenylazide-functionalized B:NCD

The 4-azidophenyl-functionalized B:NCD surface was reacted with ethynylferrocene through CuAAC click chemistry. $CuSO_4.5H_2O$ (1 mg, 4 μmol) and L-AA (1.5 mg, 8.5 μmol) were dissolved in ultrapure water (7.5 mL), while ethynylferrocene (6 mg, 28.6 μmol) was dissolved in isopropanol (7.5 mL). Next, these two solutions were mixed and the azide-terminated diamond sample was immersed in the solution mixture. The reaction vessel containing the diamond sample and the solution mixture was covered with aluminium foil to protect L-AA from light.[9] After the reaction, the diamond sample was washed and sonicated with ultrapure water to remove any unbound molecules and kept in a desiccator under vacuum.

Clicking the alkyne-terminated ss-DNA probe onto phenylazide-functionalized B:MCD

B:MCD was first modified with phenylazide groups and then the custom-synthesized alkyne-modified ss-DNA probe (Base Click) was covalently attached to it through a CuAAC click reaction.[33] For this coupling reaction, a special reaction kit for click reactions from Baseclick was used.[33] The click reaction was performed according to the protocol provided with slight modifications. The ss-DNA probe was first diluted with ultrapure water to make a 1 mM stock solution. The TBTA ligand (1 mg, 2 μmol) and CuBr (5 mg, 35 μmol) were dissolved in the reaction solvent. The diluted ss-DNA probe, the TBTA ligand and CuBr were then mixed in a reaction vessel and more reaction solvent was added until the final concentration of ss-DNA, TBTA ligand and CuBr reached 10, 30, and 15 μM respectively. A 20 μL volume of this solution mixture was then pipetted onto the 4-azidophenyl-functionalized B:MCD surface and the reaction was continued for 12 h in the dark at room temperature. After the reaction, the diamond samples were rinsed and washed thoroughly with the reaction solvent and ethanol. The ss-DNA probe-functionalized diamond samples were kept at 4 °C in PBS (phosphate buffered saline) buffer (pH 7) when they were not in use.

Hybridization

Two different types of target DNA labeled with 6-carboxyfluorescein (FAM) (Eurogentec) were used, a sequence complementary to the probe ss-DNA and a sequence with a 1-base mismatch at base pair 20 (Table 2). A 6 µL solution of DNA (100 pmol/µL) was added to 14 µL of 1 × Polymerase Chain Reaction buffer (PCR-buffer, diluted from 10 × PCR-buffer, Roche Diagnostics). This 20 µL of DNA/PCR solution was then added to the probe DNA-functionalized diamond samples and incubated at 35 °C for 2 hours. After the hybridization, the samples were first washed with 2 x SSC/0.5 % SDS, then with 0.2 × SSC at 30 °C, thereafter with 0.2 × SSC at room temperature, and finally with 1 × PBS at room temperature.[37]

Table 2. Base sequences of the probe and the corresponding full match and mismatch target DNA.

Name	Sequence
Probe DNA	5´-Alkyne-AAAAAAACCCCTGCAGCCCATGTATACCCCCGAACC-3’
Full Match (FM)	5'-FAM-GGT TCG GGG GTA TAC ATG GGC TGC AGG GG-3'
Mismatch BP 20 (MM)	5'-FAM- GGT TCG GGG **C**TA TAC ATG GGC TGC AGG GG-3'

X-ray photoelectron spectroscopy

Photoemission experiments were carried out using a Scienta ESCA 200 spectrometer in ultrahigh vacuum with a base pressure of $1x10^{-10}$ mbar. The measurement chamber is equipped with a monochromatic Al Kα X-ray source (1486.6 eV). The XPS experimental conditions were set so that the full width at half maximum of the clean Au $4f_{7/2}$ line was 0.65 eV. All spectra were measured at a photoelectron take-off angle of 0°, i.e. normal emission, and at room temperature.

Water contact angle measurements

A droplet of water (0.5 µL) was deposited onto the surface to be studied. Contact angle measurements were performed with an OCA 15 EC contact angle measuring instrument by Data Physics.

Electrochemical measurements

CV was used for the analysis of the ferrocene moieties after the click reaction. CV was carried out with an Autolab PGSTAT30 potentiostat (Eco Chemie B.V.) and controlled by the GPES Manager program. All measurements were performed in a one-compartment cell with three-electrode configuration. A sample with an area of 0.5 cm^2 was immersed into the electrolyte solution or measurement solution. The electrochemical measurements were performed in freshly distilled acetonitrile (over CaH_2). $TBAPF_6$ was added as a supporting electrolyte. The electrolytic solution was purged with N_2-gas for 5 min prior to the electrochemical measurements, eliminating traces of oxygen in the CV experiments.

Impedance spectroscopy

Impedance measurements were carried out with a home-built two electrode miniaturized impedance spectroscopy unit.[35] A transparent Perspex flow cell with an inner volume of 110 µL was used to exchange media. In this cell, the diamond sample acts as a working electrode and a gold wire (diameter 500 mm) acts as a counter electrode. The working electrode was pressed onto a copper lid using silver paste. The copper lid serves as a back electrode as well as heat sink. All impedance spectroscopy experiments were performed at the open-circuit potential with a 10 mV modulation, in PBS solution (pH 7) without any added redox agents. Under these conditions, there is no oxidation-reduction chemistry taking place, and the measurements are only measuring the intrinsic electrical properties of the interface. The full frequency spectrum of the impedimetrical data (100 Hz to 100 kHz) for DNA-modified diamond surfaces can be simulated with a 5-element circuit consisting of a resistor, representing the bulk solution inside the flow cell, in series with two complex resistors, representing the molecular layer and space-charge region, respectively.[34] This circuit is shown in Figure 14.

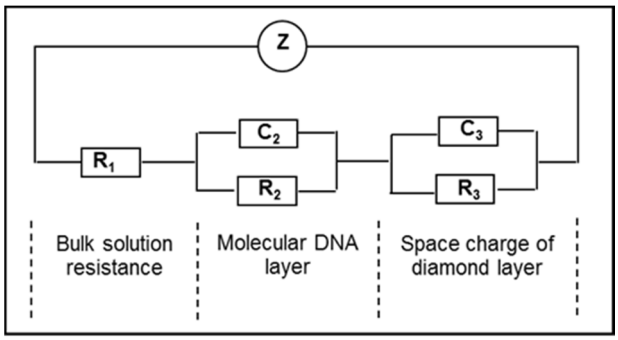

Figure 14. Circuit model used to analyze Cole-Cole plots.

Confocal microscopy

Fluorescence images were taken on a Zeiss LSM 510 META Axiovert 200 M laser scanning confocal fluorescence microscope. To excite the FAM fluorescence dye, a 488 nm argon-ion laser was used with a maximum intensity at the sample surface of 30 μW, to avoid bleaching during the image acquisition. The fluorescent intensity was collected using a long pass filter 505 nm. The following filter sets were used: MBS HFT 488, DBS NFT 490, or mirror. All images were collected with a 10×/0.3 Plan Neofluar air objective with a working distance of 5.6 mm. The image size was 225 by 225 μm². The pinhole size was 150 μm. The detector gain, being a measure for the photomultiplier voltage in arbitrary units, was set to 950. The fluorescent intensity was analyzed using ImageJ software.[37]

Acknowledgements

This work was financially supported by the Special Research Fund of Hasselt University, the Research Foundation Flanders (FWO) (G.0555.10N and G.0829.09N), and the EU FP7 Collaborative Project “MOLESOL” (No. 256617). We thank H. Penxten for the cyclic voltammetry measurements, B. Ruttens for the SEM images, and P. Robaeys for the four-point probe measurements.

References

[1] a) R. S. Balmer, J. R. Brandon, S. L. Clewes, H. K. Dhillon, J. M. Dodson, I. Friel, P. N. Inglis, T. D. Madgwick, M. L. Markham, T. P. Mollart, N. Perkins, G. A. Scarsbrook, D. J. Twitchen, A. J. Whitehead, J. J. Wilman, S. M. Woollard, *J. Phys.: Condens. Matter* **2009**, *21*, 364221-364245; b) O. Williams, M. Nesladek, in: *Physics and Applications of CVD Diamond* (Eds: S. Koizumi, C. Nebel, M. Nesladek), Wiley-VCH, Weinheim, Germany **2008**.

[2] M. Amaral, P. S. Gomes, M. A. Lopes, J. D. Santos, R. F. Silva, M. H. Fernandes, *Acta Biomater.* **2009**, *5*, 755-763.

[3] P. Scajev, S. Nargelas, K. Jarasiunas, I. Kisialiou, E. Ivakin, W. Deferme, J. D'Haen, K. Haenen, *Phys. Status Solidi A* **2013**, *210*, 2022-2027.

[4] S. D. Janssens, P. Pobedinskas, J. Vacik, V. Petrakova, B. Ruttens, J. D'Haen, M. Nesladek, K. Haenen, P. Wagner, *New J. Phys.* **2011**, *13*, 083008-083027.

[5] a) Q. Wang, P. Subramanian, M. S. Li, W. S. Yeap, K. Haenen, Y. Coffinier, R. Boukherroub, S. Szunerits, *Electrochem. Commun.* **2013**, *34*, 286-290; b) J. Shalini, Y. C. Lin, T. H. Chang, K. J. Sankaran, H. C. Chen, I. N. Lin, C. Y. Lee, N. H. Tai, *Electrochim. Acta* **2013**, *92*, 9-19.

[6] a) K. I. Sotowa, T. Amamoto, A. Sobana, K. Kusakabe, T. Imato, *Diamond Relat. Mater.* **2004**, *13*, 145-150; b) N. J. Yang, H. Uetsuka, H. Watanabe, T. Nakamura, C. E. Nebel, *Chem. Mater.* **2007**, *19*, 2852-2859; c) R. Boukherroub, X. Wallart, S. Szunerits, B. Marcus, P. Bouvier, M. Mermoux, *Electrochem. Commun.* **2005**, *7*, 937-940; d) R. E. Ruther, M. L. Rigsby, J. B. Gerken, S. R. Hogendoorn, E. C. Landis, S. S. Stahl, R. J. Hamers, *J. Am. Chem. Soc.* **2011**, *133*, 5692-5694; e) S. A. Yao, R. E. Ruther, L. H. Zhang, R. A. Franking, R. J. Hamers, J. F. Berry, *J. Am. Chem. Soc.* **2012**, *134*, 15632-15635; f) T. Nakamura, T. Ohana, *Jpn. J. Appl. Phys.* **2012**, *51*, 085201-085206.

[7] a) A. Härtl, E. Schmich, J. A. Garrido, J. Hernando, S. C. R. Catharino, S. Walter, P. Feulner, A. Kromka, D. Steinmüller, M. Stutzmann, *Nat. Mater.* **2004**, *3*, 736-742; b) W. S. Yang, O. Auciello, J. E. Butler, W. Cai, J. A. Carlisle, J. Gerbi, D. M. Gruen, T. Knickerbocker, T. L. Lasseter, J. N. Russell, L. M. Smith, R. J. Hamers, *Nat. Mater.* **2002**, *1*, 253-257; c) K. Y. Tse, B. M. Nichols, W. S. Yang, J. E. Butler, J. N. Russell, R. J. Hamers, *J. Phys. Chem. B* **2005**, *109*, 8523-8532; d) X. Wang, P. E. Colavita, K. M. Metz, J. E. Butler, R. J. Hamers, *Langmuir* **2007**, *23*, 11623-11630.

[8] X. Y. Wang, E. C. Landis, R. Franking, R. J. Hamers, *Acc. Chem. Res.* **2010**, *43*, 1205-1215.

[9] M. R. Das, M. Wang, S. Szunerits, L. Gengembre, R. Boukherroub, *Chem. Commun.* **2009**, 2753-2755.

[10] M. Wang, M. R. Das, M. S. Li, R. Boukherroub, S. Szunerits, *J. Phys. Chem. C* **2009**, *113*, 17082-17086.

[11] H. Notsu, T. Tatsuma, A. Fujishima, in *Diamond Electrochemistry* (Eds.: A. Fujishima, Y. Einaga, T. N. Rao, D. A. Tryk), Elsevier, Amsterdam **2005**, pp. 218-237.

[12] C. Agnès, S. Ruffinatto, E. Delbarre, A. Roget, J. C. Arnault, F. Omnès, P. Mailley, *IOP Conf. Series: Materials Science and Engineering* **2010**, *16*, 012001-012012.

[13] a) W. Jian, M. A. Firestone, O. Auciello, J. A. Carlisle, *Langmuir* **2004**, *20*, 11450-11456; b) S. Q. Lud, M. Steenackers, R. Jordan, P. Bruno, D. M. Gruen, P. Feulner, J. A. Garrido, M. Stutzmann, *J. Am. Chem. Soc.* **2006**, *128*, 16884-16891; c) Y. L. Zhong, W. Ng, J. X. Yang, K. P. Loh, *J. Am. Chem. Soc.* **2009**, *131*, 18293-18298; d) C. Agnès, J. C. Arnault, F. Omnès, B. Jousselme, M. Billon, G. Bidan, P. Mailley, *Phys. Chem. Chem. Phys.* **2009**, *11*, 11647-11654.

[14] Y. L. Zhong, K. P. Loh, A. Midya, Z. K. Chen, *Chem. Mater.* **2008**, *20*, 3137-3144.

[15] D. Belanger, J. Pinson, *Chem. Soc. Rev.* **2011**, *40*, 3995-4048.

[16] A. Mesnage, X. Lefevre, P. Jegou, G. Deniau, S. Palacin, *Langmuir* **2012**, *28*, 11776-11787.

[17] Z. W. Zhu, Y. Wang, X. Zhang, C. F. Sun, M. G. Li, J. W. Yan, B. W. Mao, *Langmuir* **2012**, *28*, 14739-14746.

[18] X. S. Zhou, Z. R. Dong, H. M. Zhang, J. W. Yan, J. X. Gao, B. W. Mao, *Langmuir* **2007**, *23*, 6819-6826.

[19] D. K. Aswal, S. Lenfant, D. Guerin, J. V. Yakhmi, D. Vuillaume, *Anal. Chim. Acta* **2006**, *568*, 84-108.

[20] a) M. Grätzel, *Nature* **2001**, *414*, 338-344; b) C. V. Subban, M. Ati, G. Rousse, A. M. Abakumov, G. Van Tendeloo, R. Janot, J. M. Tarascon, *J. Am. Chem. Soc.* **2013**, *135*, 3653-3661; c) B. Dunn, H. Kamath, J. M. Tarascon, *Science* **2011**, *334*, 928-935.

[21] I. Willner, E. Katz, *Angew. Chem. Int. Ed.* **2000**, *39*, 1180-1218.

[22] J. Lahann, in: *Click Chemistry for Biotechnology and Materials Science* (Ed. J. Lahann), John Wiley & Sons Ltd., West Sussex **2009**, pp.1-8.

[23] B. L. Frey, R. M. Corn, *Anal. Chem.* **1996**, *68*, 3187-3193.

[24] H. C. Kolb, M. G. Finn, K. B. Sharpless, *Angew. Chem. Int. Ed.* **2001**, *40*, 2004-2021.

[25] R. M. Arnold, J. Locklin, *Langmuir* **2013**, *29*, 5920-5926.

[26] C. Grabosch, M. Kind, Y. Gies, F. Schweighofer, A. Terfort, T. K. Lindhorst, *Org. Biomol. Chem., OBC* **2013**, *11*, 4006-4015.

[27] C. P. Andrieux, J. Pinson, *J. Am. Chem. Soc.* **2003**, *125*, 14801-14806.

[28] R. D. Rohde, H. D. Agnew, W. S. Yeo, R. C. Bailey, J. R. Heath, *J. Am. Chem. Soc.* **2006**, *128*, 9518-9525.

[29] J. P. Collman, N. K. Devaraj, C. E. D. Chidsey, *Langmuir* **2004**, *20*, 1051-1053.

[30] A. J. Bard, L. R. Faulkner, *Electrochemical Methods: Fundamentals and Applications*, John Wiley & Sons Inc., New York, **2001**.

[31] T. Kondo, H. Hoshi, K. Honda, Y. Einaga, A. Fujishima, T. Kawai, *J. Phys. Chem. C* **2008**, *112*, 11887-11892.

[32] A. M. Napper, H. Y. Liu, D. H. Waldeck, *J. Phys. Chem. B* **2001**, *105*, 7699-7707.

[33] M. Coates, T. Nyokong, *J. Electrochem. Soc.* **2012**, *687*, 111-116.

[34] P. M. E. Gramlich, C. T. Wirges, A. Manetto, T. Carell, *Angew. Chem. Int. Ed.* **2008**, *47*, 8350-8358.

[35] W. S. Yang, J. E. Butler, J. N. Russell, R. J. Hamers, *Langmuir* **2004**, *20*, 6778-6787.

[36] a) B. van Grinsven, T. Vandenryt, S. Duchateau, A. Gaulke, L. Grieten, R. Thoelen, S. Ingebrandt, W. De Ceuninck, P. Wagner, *Phys. Status Solidi A* **2010**, *207*, 919-923; b) B. van Grinsven, N. Vanden Bon, L. Grieten, M. Murib, S. D. Janssens, K. Haenen, E. Schneider, S. Ingebrandt, M. J. Schöning, V. Vermeeren, M. Ameloot, L. Michiels, R. Thoelen, W. De Ceuninck, P. Wagner, *Lab Chip* **2011**, *11*, 1656-1663.

[37] T. Y. Lee, Y. B. Shim, *Anal. Chem.* **2001**, *73*, 5629-5632.

[38] M. S. Murib, B. van Grinsven, L. Grieten, S. D. Janssens, V. Vermeeren, K. Eersels, J. Broeders, M. Ameloot, L. Michiels, W. De Ceuninck, K. Haenen, M. J. Schöning, P. Wagner, *Phys. Status Solidi A* **2013**, *210*, 911-917.

[39] K. Arihara, A. Fujishima, Central Japan Railway Company, EP1754804 A1, **2005**.

[40] W. Gajewski, P. Achatz, O. A. Williams, K. Haenen, E. Bustarret, M. Stutzmann, J. A. Garrido, *Phys. Rev. B* **2009**, *79*, 045206.

[41] a) A. E. Fischer, Y. Show, G. M. Swain, *Anal. Chem*. **2004**, *76*, 2553-2560; b) E. Vanhove, J. de Sanoit, J. C. Arnault, S. Saada, C. Mer, P. Mailley, P. Bergonzo, M. Nesladek, *Phys. Status Solidi A* **2007**, *204*, 2931-2939.

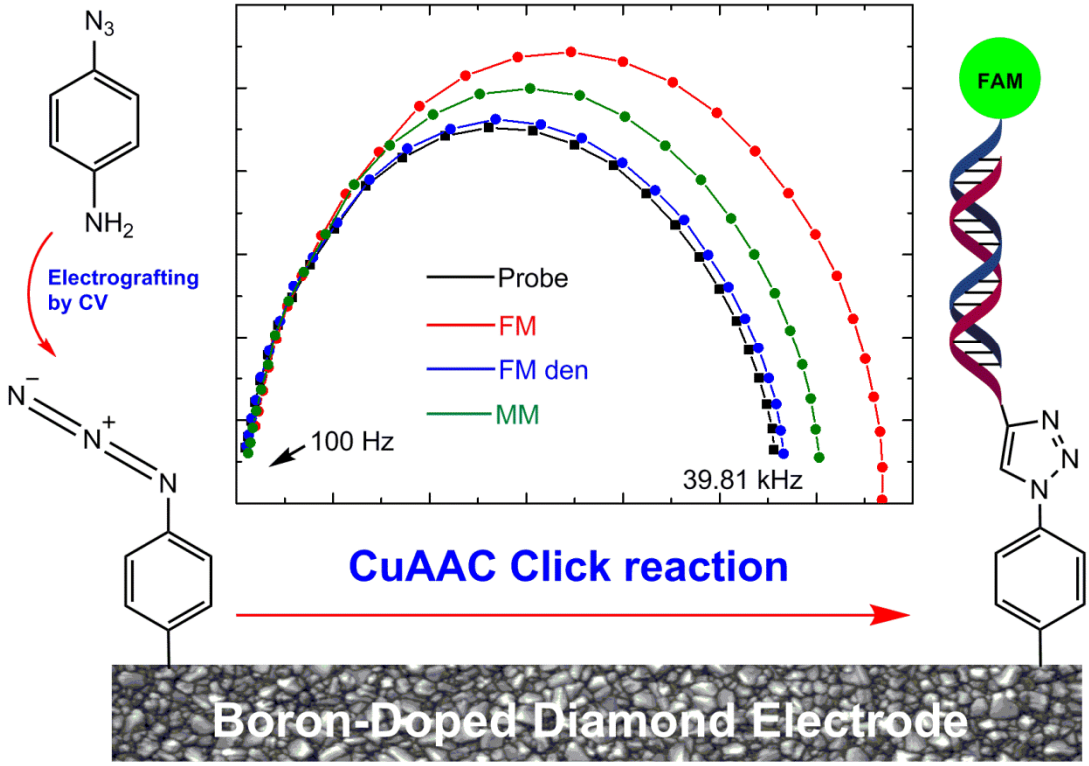

Efficient surface functionalization of boron-doped diamond electrodes via a combination of diazonium electrografting and CuAAC click chemistry is presented. The applicability of the functionalization approach for DNA sensing is demonstrated by covalent coupling with ss-DNA and evaluation by impedance spectroscopy.